MINERALOGICAL MAGAZINE, VOL. 45, 1982, PP. 47–54

Amphiboles in the Lilloise intrusion, East Greenland

P. E. BROWN AND F. E. TOCHER
Department of Geology and Mineralogy, The University, Aberdeen AB9 1AS

AND

A. D. CHAMBERS
Department of Geological Sciences, University of Aston, Birmingham B4 7ET

ABSTRACT. Amphibole in the lower parts of the Lilloise layered intrusion occurs interstitially and as a replacement of pyroxene; in the upper rocks it is a major cumulus phase. There is an overall trend of increasing Fe/(Fe+Mg) with height. Coupled substitutions which effect the variation in composition of the amphiboles are chiefly Na,K(A)+Al(T) for $\square A$+Si(T) and Ti+Al(T) for Fe^{3+}(C)+Si(T). There is considerable variation in composition both on the specimen scale and within individual grains. This variation, plus scatter found in plots of the coupled substitutions, is partly attributed to many of the amphiboles having replaced pyroxene and also to the effects of magmatic-hydrothermal fluids.

THE Lilloise layered intrusion is one of the major Tertiary plutonic centres in East Greenland. It is a high-level, epizonal intrusion which cuts the regional flood basalts about 120 km east of the Skaergaard intrusion and 20 km inland from the Blosseville coast (fig. 1). The 5 × 9 km outcrop is in difficult country and the eventual success of attempts to gain access to the intrusion owed much to the encouragement of Professor W. A. Deer. Reconnaissance observations were made by Brown (1973) and Matthews (1976) and more detailed evidence concerning the efflux of magmatic water from the intrusion into its contact aureole was presented by Sheppard *et al.* (1977). The present paper is concerned with variations in amphiboles which form an important intercumulus phase in the lower parts of the intrusion and a major cumulus phase higher up.

General geology. After an initially quiet period of crystallization and at a late stage of consolidation of the layered series, the Lilloise intrusion underwent considerable internal subsidence which caused great disturbance of the layering. In particular an uppermost unit of plagioclase–amphibole cumulates now forms a tight syncline which is superbly displayed in a 500 m-high cliff referred to as the White Wall. Despite this disturbance of the original igneous stratigraphy, a total thickness of at least 3000 m of layered rocks is exposed and there is extensive cryptic and mineralogical variation (fig. 2). The lowest exposed cumulates are of olivine–clinopyroxene–chrome spinel, above which are olivine–clinopyroxene–plagioclase–Fe-Ti oxide cumulates, which in turn are overlain by the plagioclase–amphibole cumulates that form the topmost preserved part of the layered sequence.

The amphiboles. In the lowest rocks amphibole is present as a very minor and irregularly developed patchy replacement of cumulate clinopyroxene and less commonly as an interstitial phase. Higher up in the plagioclase-bearing cumulates amphibole is more conspicuous, mainly as a patchy replacement of clinopyroxene, but also interstitially and as rims

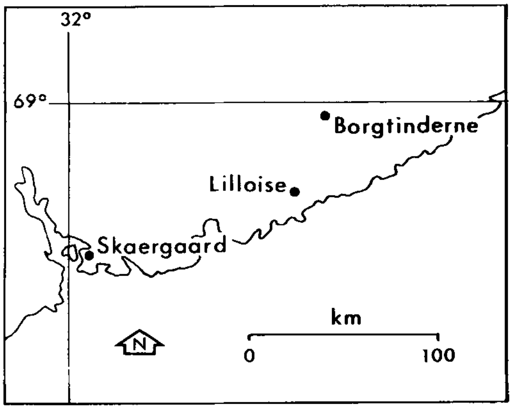

FIG. 1. Location of the Lilloise Intrusion on the Blosseville coast of East Greenland.

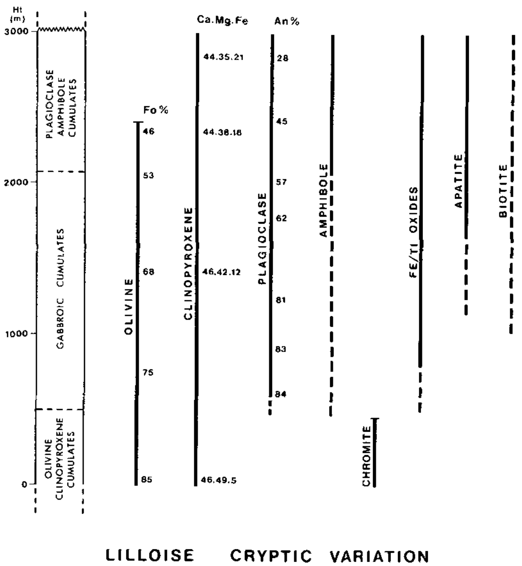

FIG. 2. Summary diagram of mineralogy and cryptic variation. Continuous vertical lines indicate cumulus phases.

to clinopyroxene or opaque oxides. In the upper part of the intrusion, as exposed in the White Wall, large elongated cumulate amphiboles form up to half of the more mafic parts of some spectacular layered and laminated rocks. The amphiboles are typically pleochroic in shades of red-brown.

Microprobe analyses of the amphiboles were made using a Link EDS attachment to a Cambridge Instruments Geoscan. A limited number of wavelength-dispersive analyses are also incorporated in the data. Representative compositions (Table I) illustrate the main features of the amphibole chemistry, but the bulk of the data for the 140 analyses used is presented graphically. In the absence of water determinations the analyses were computer-reduced on the basis of 23 oxygen atoms and the formulae calculated according to the recommendations of the IMA Subcommittee on Amphiboles (Leake, 1978), i.e. writing the standard formula

$$A_{0-1}\,B_2\,C_5^{\mathrm{vi}}\,T_8^{\mathrm{iv}}\,\mathrm{O}_{22}(\mathrm{OH})_2$$

(*a*) Sum T to 8 using Si, then Al,Cr^{3+},Fe^{3+},Ti^{4+}, in order.
(*b*) Sum C to 5 using excess Al,Cr,Ti,Fe^{3+} from (*a*), then Mg, then Fe^{2+}, and then Mn.
(*c*) Sum B to 2 using excess Fe^{2+},Mn,Mg from (*b*), then Ca, then Na.
(*d*) Excess Na from (*c*) is assigned to A, then all K. Total A should be between 0.00 and 1.00 inclusive.

Previous accurate determinations of $\mathrm{H_2O^+}$ in Lilloise amphiboles used for oxygen and hydrogen isotope analyses (Sheppard *et al.*, 1977) ranged between 1.49 and 1.69 wt. %.

As the microprobe does not distinguish ferric from ferrous iron, calculation of structural formulae on the basis of zero Fe^{3+} represents the least departure from the data and this procedure was one of those adopted. Alternatively, analyses of bulk separates of amphiboles from several specimens of plagioclase-amphibole cumulates indicated an average Fe^{3+} content equivalent to about 20% of the total iron as Fe^{2+} and the structural formulae were also calculated using this figure throughout. Where appropriate the results of both methods of calculation will be compared and discussed. There are obvious pitfalls in applying a uniform 20% Fe^{3+} content in that the oxidation ratio of the iron in the amphiboles almost certainly varies through the layered series and indeed, in the amphibole cumulates themselves, uniform application of this figure is a generalization.

The report of the IMA Subcommittee on Amphiboles (Leake, 1978) suggested alleviation of the iron oxidation problem for microprobe analyses by varying $\mathrm{Fe}^{2+}/\mathrm{Fe}^{3+}$ to make the total number of cations, excluding (Ca + Na + K), equal to 5 + 8; in an addendum to that report B. E. Leake and M. H. Hey recommended the alternative procedure of calculating on the basis of 13 cations (excluding (Ca + Na + K)) and adjusting $\mathrm{Fe}^{2+}/\mathrm{Fe}^{3+}$ to bring O to 23. For the Lilloise amphiboles neither procedure gave values that were sufficiently consistent with those obtained wet chemically. Consequently,

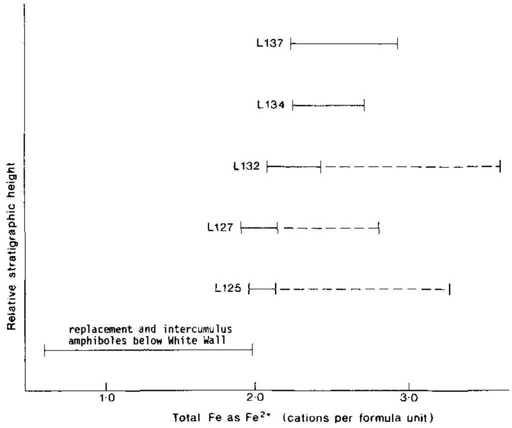

FIG. 3. Range of total Fe^{2+} in the amphiboles of the amphibole-plagioclase cumulates, arranged in ascending stratigraphic order. Solid lines indicate major range and dotted lines extremes of variation.

TABLE I. *Representative electron microprobe (EDS) analyses and cations per 23 oxygen atoms for amphiboles from the Lilloise intrusion. (Total iron as* Fe^{2+}*)*

	L114 AM 2	L116 AM 2/2	L113 AM 3	L189 AM 4	L125 AM 1C	L132 AM 2R	L134 AM 3	L137 AM 2R
SiO_2	40.43	49.37	41.03	40.91	40.43	40.80	42.55	40.90
TiO_2	4.78	1.40	4.30	4.23	4.34	3.58	2.33	3.42
Al_2O_3	13.36	6.73	12.43	11.66	11.40	11.92	10.00	11.20
FeO	9.70	12.90	13.89	15.78	16.76	17.54	19.31	18.85
MnO	—	0.24	0.16	0.21	0.33	0.24	0.36	0.36
MgO	13.36	14.91	11.01	10.73	9.92	9.47	9.15	8.77
CaO	12.33	11.96	11.82	11.60	11.28	11.31	11.57	11.63
Na_2O	2.11	0.95	2.34	2.31	2.28	2.23	1.99	1.78
K_2O	0.81	0.31	0.95	0.75	1.12	0.92	0.84	1.05
Total	96.88	98.77	97.93	98.18	97.86	98.01	98.10	97.96
Si	5.981	7.103	6.119	6.137	6.133	6.177	6.471	6.241
Al	2.019	0.897	1.881	1.863	1.867	1.823	1.529	1.759
ΣT site	8.000	8.000	8.000	8.000	8.000	8.000	8.000	8.000
Al	0.312	0.243	0.305	0.199	0.171	0.305	0.264	0.255
Ti	0.532	0.151	0.482	0.477	0.495	0.407	0.266	0.392
Mg	2.945	3.197	2.448	2.400	2.241	2.137	2.074	1.993
Fe^{2+}	1.200	1.408	1.733	1.942	2.092	2.151	2.396	2.360
Mn	—	—	0.020	—	—	—	—	—
ΣC site	4.989	4.999	4.988	5.000	5.000	5.000	5.000	5.000
Fe^{2+}	—	0.143	—	0.056	0.034	0.070	0.059	0.046
Mn	—	0.029	—	0.027	0.042	0.031	0.046	0.047
Ca	1.954	1.844	1.889	1.865	1.833	1.835	1.886	1.901
Na	0.046	—	0.111	0.053	0.091	0.065	0.008	0.006
ΣB site	2.00	2.016	2.000	2.000	2.000	2.000	2.000	2.000
Na	0.558	0.264	0.566	0.620	0.580	0.591	0.578	0.522
K	0.153	0.057	0.180	0.143	0.216	0.177	0.163	0.204
ΣA site	0.711	0.321	0.746	0.763	0.796	0.768	0.741	0.726

data are presented as outlined above and only when discussing relevant coupled substitutions and other specific points is the probable significance of Fe^{3+} variation discussed. Calculating Fe^{3+} as Fe^{2+} results in slight inaccuracies in other cation and site totals. However, as wet chemical analysis suggests that Fe^{3+} is never high, distortions due to this are of minor significance, even for Si,Al^T,Al^C and *A*-site total, those parameters most strongly affected.

Amphibole chemistry. One of the dominant chemical characteristics of the amphiboles is a high content of Ti which in the majority of analyses is more than 0.4 cations per structural formula. Using the IMA recommendations on nomenclature, and Fe^{3+} as 20% of the total Fe^{2+}, the microprobe analyses fall in the range pargasite, hastingsite, and kaersutite (where the Ti content exceeds 0.5 cations), with prefix variations according to Mg/(Mg + Fe) ratios; there are also a few analyses with Si cations between 6.25 and 6.50 which earn the additional accolade of hornblende. With zero Fe^{3+} the amphiboles become dominantly ferroan pargasites and kaersutites.

The microprobe analyses reveal great variation, both within section and within grain, but an important change in the amphiboles with height in the layered series is increase in iron. Representative specimens from the sequence of plagioclase–amphibole cumulates on the White Wall show this increase and an extensive within-specimen spread in the analyses (fig. 3). The variation is mainly accounted for by the exchange $Mg \rightleftharpoons Fe^{2+}$ although variation in Fe^{3+}, expressed as Fe^{2+}, may be a factor. Over the full range of analyses of interstitial, replacement and cumulus amphiboles, the Fe/(Fe + Mg) extremes are 0.134 to 0.788. Variation of Fe/(Fe + Mg) in coexisting clinopyroxenes

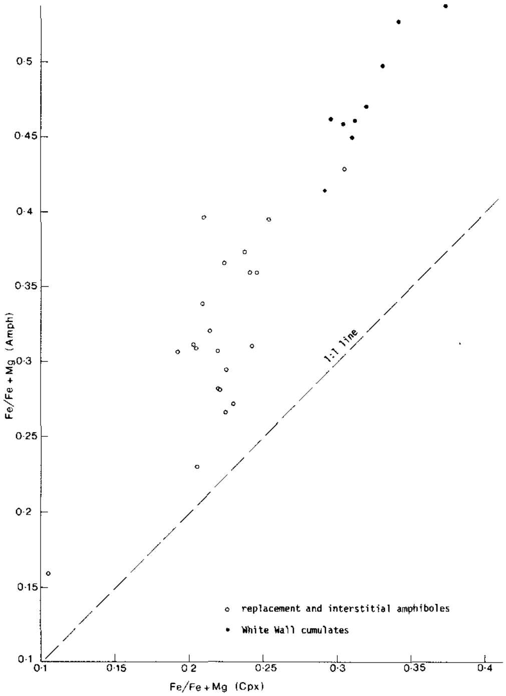

FIG. 4. Structural formulae Fe/(Fe+Mg) in coexisting amphiboles and clinopyroxenes (total Fe as Fe^{2+}). Each point represents an average of available analyses for a rock specimen. The 1:1 line is indicated for reference.

(fig. 4) shows positive correlation with that in the amphiboles, scatter tending to be greater for the replacement amphiboles as compared with the cumulus amphiboles.

Other simple exchange reactions are $Mn \rightleftharpoons Mg$ and $Na \rightleftharpoons K$. Ca shows little variation and the ratio Na/(Na+Ca) in both replacement and cumulus amphiboles does not vary greatly with change in composition of the coexisting plagioclase (fig. 5), although the lowest values are found in rocks with the most calcic plagioclase.

Other more complex variations in Si, Al, Ti, and alkalis involve coupled substitutions.

Coupled substitutions. To assess the importance of coupled substitutions computer plots were made on the basis of structural formulae derived from the 140 microprobe analyses. Our treatment of the substitutions follows the discussions by Robinson *et al.* (1971), Helz (1973), and Czamanske and Wones (1973). In the plots, since both co-ordinates are subject to errors of the same sort of magnitude, the reduced major axis line has been taken as the best fit.

Si values show significant variation in the Lilloise amphiboles. With increasing Si there is a significant decrease in Al and related increases in Na, K, and Ti. Ca shows no appreciable variation. The more important coupled substitutions to which these changes may be linked are:

1. $Na,K(A) + Al(T)$ for $\square(A) + Si(T)$ (Edenite).
2. $Al,Fe^{3+}(C) + Al(T)$ for $Mg,Fe(C) + Si(T)$ (Tschermakite).
3. $Ti(C) + 2Al(T)$ for $Mg,Fe(C) + 2Si(T)$ (Ti-tschermakite).
4. $Ti(C) + Al(T)$ for $Al,Fe^{3+}(C) + Si(T)$.

Robinson *et al.* (1971) noted that a combination of substitutions 1, 2, and 3 should yield a 1:1 slope when $A\text{-site} + Al(C) + Fe^{3+}(C) + 2Ti^{4+}$ is plotted against Al(*T*). Figs. 6 and 7 respectively show this correlation for zero Fe^{3+} and Fe^{3+} as 20% of the total iron. The inclusion of Fe^{3+} marginally improves the correlation coefficient, but in both cases the slope of the reduced major axis line is about 35° with a positive intercept on the Al(*T*) axis.

Plotting $A\text{-site} + Al(C) + Fe^{3+}(C) + Ti^{4+}$ *vs.* Al(*T*), a combination of substitutions 1, 2, and 4, effects a significant improvement. At zero Fe^{3+} (fig. 8), the reduced major axis line has a 47° slope and an 0.94 correlation coefficient, but is somewhat offset towards an excess of Al(*T*). With Fe^{3+} as 20% of the total Fe^{2+} the correlation remains good and the excess of Al(*T*) is reduced.

Individual components of these combinations of substitutions can now be examined. Correlation between total *A*-site occupancy and Al(*T*) (substitution 1) is moderate and only a slight improvement is effected by plotting total *A*-site–Na(*B*) against Al(*T*) (fig. 9). Subtracting Na(*B*) removes any effect of the substitution $Na(A) + Na(B) \rightleftharpoons \square A + Ca(B)$ (Richterite) (cf. Czamanske and Wones, 1973), but this substitution is in any case of little importance, as indicated by the minor variation found in Ca. The slope of the reduced major axis line for the data in fig. 9 indicates a ratio of substitution of Al in the *T*-site to substitution in the *A*-site of about 2:1, showing that Al(*T*) is involved in further

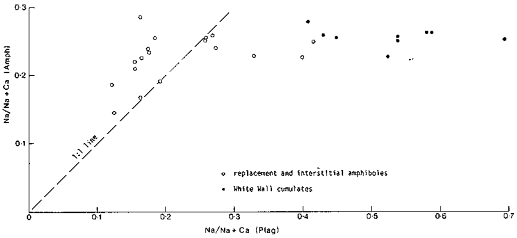

FIG. 5. Structural formulae Na/(Na+Ca) in coexisting amphiboles and plagioclases. Each point represents an average of available analyses for a rock specimen. The 1:1 line is indicated for reference.

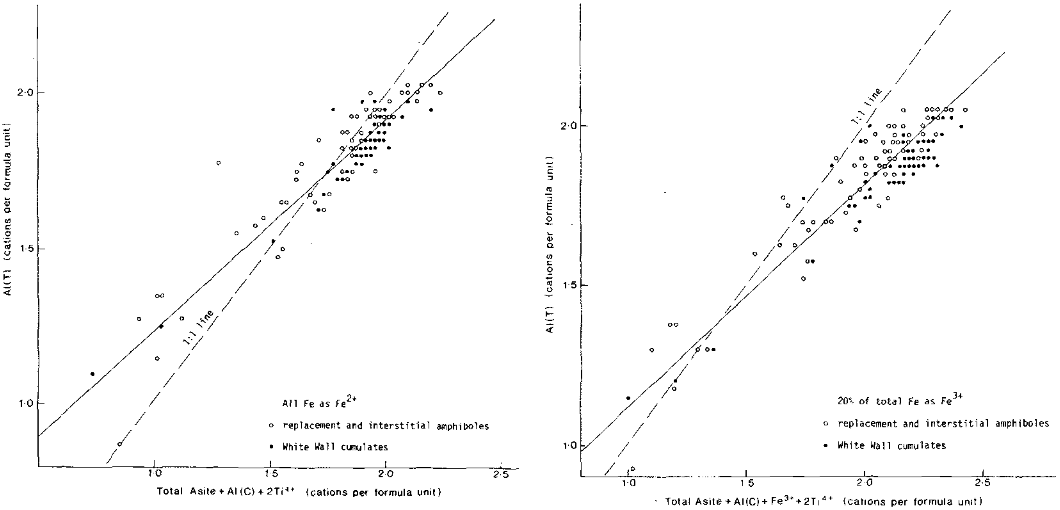

FIGS. 6 and 7. FIG. 6. (*left*). Total A-site + Al(C) + 2Ti *vs.* Al(T). Structural formulae calculated with zero Fe^{3+}. This and other diagrams drawn from computer print-outs which do not distinguish overlapping points. Predicted 1 : 1 slope shown by dashed line. Reduced major axis line shown continuous; $y = 0.57 + 0.68x$, correlation coefficient 0.918. FIG. 7 (*right*). Total A-site + Al(C) + Fe^{3+}(C) + 2Ti *vs.* Al(T). 20% of total Fe converted to Fe^{3+}. Reduced major axis line shown continuous; $y = 0.44 + 0.69x$, correlation coefficient 0.930.

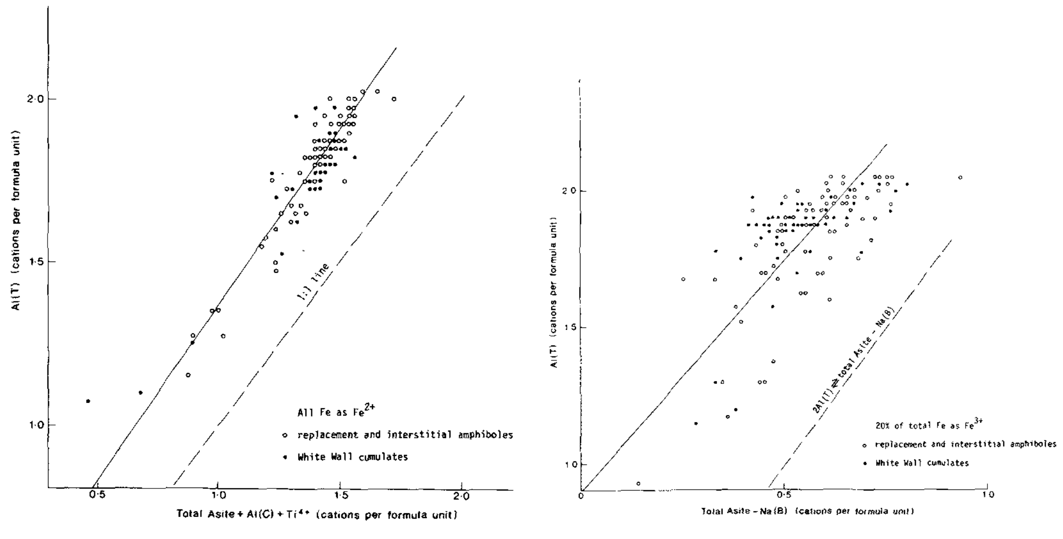

FIGS. 8 and 9. FIG. 8 (*left*). Total A-site + Al(C) + Ti *vs.* Al(T). Zero Fe^{3+}. Reduced major axis line shown continuous; $y = 0.268 + 1.091x$, correlation coefficient 0.941. With 20% of the Fe converted to Fe^{3+}, this becomes $y = 0.11 + 1.067x$, correlation coefficient 0.917. FIG. 9 (*right*). Total A-site − Na(B) *vs.* Al(T). 20% of total Fe converted to Fe^{3+}. Reduced major axis line shown continuous; $y = 0.91 + 1.68x$, correlation coefficient 0.664. With zero Fe^{3+} this becomes $y = 0.47 + 2.04x$, correlation coefficient 0.753.

coupled substitutions in addition to substitution 1 (edenite).

Plotting Al(total) against Al(*T*) produces very good correlation for both zero Fe^{3+} and Fe^{3+} present (fig. 10). In both cases the best fit line shows a modest excess of total Al over Al(*T*), this excess being Al in the *C*-site. This Al(*C*) varies only slightly over the whole range of compositions and the small divergence of the best fit line from 1Al(total) : 1Al(*C*) indicates that substitution 2 (Al-tschermakite) effects little change. Although in general the inclusion of Fe^{3+} in the computations improves the correlations being sought, the artificiality of applying a uniform percentage precludes its realistic assessment as a component of substitution 2.

Coupled substitution involving Ti is one of the major features of the amphibole variation and the total range of Ti atoms per unit formula is from 0.054 to 0.633, although a majority fall between 0.40 and 0.55. All the Ti is in the *C*-site. Correlation of Ti *vs.* Al(*T*) (substitutions 3 and 4) is virtually identical for both structural formulae with Fe^{3+} either zero or 20% of the total Fe^{2+} (fig. 11). The slope of the reduced major axis line indicates a substitution involving Al(*T*) and Ti with an Al to Ti ratio of 1.67 : 1. This ratio is consistent with the operation of coupled substitutions 1 and 2. If substitution 3 were the sole substitution operative, the Al to Ti ratio would be 2 : 1 and the additional coupled substitution involving Al(*T*) and *A*-site occupancy would increase the ratio still further. Again it is difficult to assess the role of $Fe^{3+}(C)$ in relation to changing Ti(*C*) in the overall substitution Ti(*C*) + Al(*T*) for Al,$Fe^{3+}(C)$ + Si(*T*), but as Al(*C*) hardly varies it is likely that the more relevant *C*-site change is $Ti^{4+} \rightleftharpoons Fe^{3+}$.

In considering the scatter on the plots of these substitutions it is interesting to note the findings of Helz (1973) in a hydrothermal experimental study of amphiboles in basaltic melts. With changing temperature Al(*C*) and Ti varied independently of each other so that neither varied strictly linearly with Al(*T*), although the sum (Al(*C*) + 2Ti) did. Helz did not enlarge on the significance of this observation.

Other possible substitutions, notably those involving Na(*B*) and Ca, do not produce significant correlations, as for example

Na(*B*) + Al(*C*) for Ca(*B*) + Mg(*C*) (Glaucophane)
Na(*B*) + $Fe^{3+}(C)$ for Ca(*B*) + Mg(*C*) (Riebeckite),

both of which result in plots with excessive scatter. The richterite substitution, Na(*A*) + Na(*B*) for □ + Ca(*B*), also reveals excessive variation in Na(*B*). Possibly some of this failure to find a significant pattern of behaviour for Na(*B*), and also some scatter found in plotting other substitutions, may be attributed to the evolution of high-temperature magmatic–hydrothermal fluids late in the crystallization history of the intrusion (Sheppard *et al.*, 1977). Efflux of these fluids may have effected some redistribution, notably of the alkali elements.

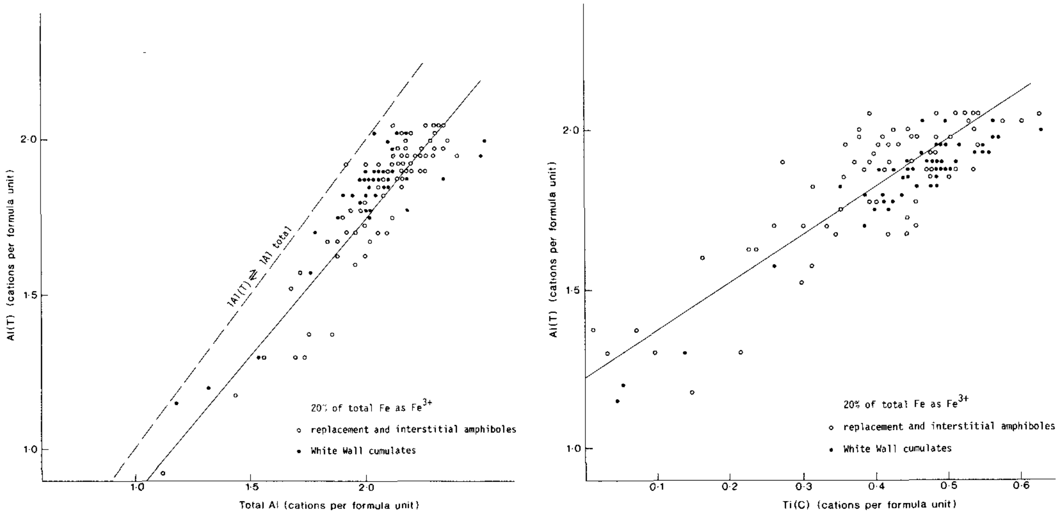

FIGS. 10 and 11. FIG. 10 (*left*). Total Al *vs.* Al(*T*). 20% of total Fe converted to Fe^{3+}. Reduced major axis line shown continuous; $y = 0.08 + 0.93x$, correlation coefficient 0.890. With zero Fe^{3+} this becomes $y = 0.16 + 0.94x$, correlation coefficient 0.894. FIG. 11 (*right*). Ti(*C*) *vs.* Al(*T*). 20% of total Fe converted to Fe^{3+}. Reduced major axis line $y = 1.14 + 1.67x$. With zero Fe^{3+} this becomes $y = 1.08 + 1.69x$, correlation coefficient 0.844.

Conclusions. Systematic variation in the Lilloise amphiboles is thus mainly accounted for by the simple substitutions of the $Fe^{2+} \rightleftharpoons Mg$ type and the coupled substitutions

$$Ti(C) + Al(T) \text{ for } Fe^{3+}(C) + Si(T)$$
$$Na,K(A) + Al(T) \text{ for } \square A + Si(T)$$

with minor contributions from

$$Al(C) + Al(T) \text{ for } Mg(C) + Si(T)$$

and possibly

$$Ti(C) + 2Al(T) \text{ for } Mg(C) + 2Si(T).$$

The range of these substitutions is very similar for both the cumulate amphiboles and the replacement and interstitial varieties. Furthermore the substitutions show a wide range on the scale of a single specimen and considerable variation on the single grain scale. Domain variation within grains was found by Czamanske and Wones (1973) in the amphiboles of the Finnmarka granodiorite and was attributed by them to adjustment to a changing magmatic environment wherein some areas of grains were more intimately interacting with the system than others.

The variables likely to have controlled the coupled substitutions are those discussed by Helz (1973) with respect to amphiboles in basaltic melts where it was found that:

the Al-tschermakite substitution had an irregular temperature dependence;

the Ti-tschermakite substitution had a positive temperature dependence, decreased with increasing f_{O_2} and possibly varied with bulk melt composition;

the edenite substitution had a positive temperature dependence and varied with bulk composition.

Estimation of the relative importance of these variables is difficult.

In the Lilloise intrusion Ti substitution is particularly important, but there is no evidence of such strongly oxidizing conditions as those which pertained in the Finmarka intrusion (Czamanske and Wones, 1973) where Fe/(Fe + Mg) in the ferromagnesian minerals decreased with progressive differentiation and f_{O_2} was a major factor controlling Ti substitution. Evolution of the late magmatic–hydrothermal system at Lilloise postdated the crystallization of the cumulates, in which the ferromagnesian minerals have increasing Fe/(Fe + Mg), and any oxidizing conditions resulting from disassociation of this fluid would be superimposed on the existing cumulus pile. This event could nevertheless have contributed significantly both to the trends of the substitution and to their seemingly fickle development.

The scatter found in plots of individual components of the combined substitutions which operated in the Lilloise amphiboles is in contrast to the findings of Czamanske and Wones for the Finnmarka granodiorite. There the amphiboles are marked by patchy domains of very different Al, Ti, and Na, but the separate substitutions plot in an exemplary linear fashion. As noted above, however, Helz did find experimental evidence of non-linear behaviour of Al(C) and Ti with Al(T). We are inclined to attribute much of the departure from linearity found in the Lilloise amphibole substitutions to the post-cumulus-deposition effects of the magmatic–hydrothermal system and to the fact that many amphiboles replace pre-existing pyroxenes.

The amphiboles which partially replace pyroxenes probably grew at an early stage of the consolidation of the lower part of the cumulus pile and at the same stage as the crystallization of the interstitial amphiboles. This would take place with falling temperature but in local micro-environments so that not only did the amphibole grains themselves react inhomogeneously to the changing conditions but the local 'magmatic' conditions may well have varied from one micro-environment to another.

Evidence suggesting the influence of micro-environments and the effect of pre-existing pyroxenes on replacement amphiboles may be seen in fig. 4, where the Fe/(Fe + Mg) ratio of coexisting amphiboles and pyroxenes has a greater spread in the replacement than the cumulus amphiboles. Also, although not plotted, it may be noted that there is little systematic variation of Ti in coexisting amphiboles and pyroxenes and there is considerable within-specimen spread of Ti values. Most amphiboles have significantly higher Ti contents than the pyroxenes, even when they replace the latter, and the amphibole Ti may have been controlled by Fe–Ti oxides in individual micro-environments. Similarly, although the Na/(Na + Ca) ratios in the amphiboles show little change (fig. 5), the lowest values (and the greatest spread of values in individual specimens) are found in rocks with cumulus Ca-rich plagioclase where the amphibole occurs as replacement patches in pyroxene or along grain boundaries.

Although similar trends are found in the cumulate amphiboles, they show less departure from linearity than the replacement types and this may be due to their having crystallized in a more open magmatic environment. Even in the cumulate amphiboles, however, occasional grains bear telltale signs of a remnant pyroxene core and this could be a factor contributing to some of the variations found.

In conclusion it may be noted that there is considerable overlap of the composition of the Lilloise amphiboles, notably in Al, Ti, and K, with the field of amphiboles of possible mantle origin (Best, 1970, 1974). Much remains to be established concerning kaersutitic amphiboles as potentially useful geobarometers.

Acknowledgements. Financial support from the Royal Society, the NERC and the Carnegie Trust is gratefully acknowledged. Dr I. Parsons kindly commented on the manuscript.

REFERENCES

Best, M. G. (1970) *Contrib. Mineral. Petrol.* **27,** 25–44.
——(1974) *J. Geophys. Res.* **79,** 2107–13.
Brown, P. E. (1973) *J. Geol. Soc.* **129,** 405–18.
Czamanske, G. K., and Wones, D. R. (1973) *J. Petrol.* **14,** 349–80.
Helz, R. T. (1973) Ibid. **14,** 249–302.
Leake, B. E. (1978) *Mineral. Mag.* **42,** 533–63.
Matthews, D. W. (1976) *Geol. Mag.* **113,** 287–95.
Robinson, P., Ross, M., and Jaffe, H. W. (1971) *Am. Mineral.* **56,** 1005–41.
Sheppard, S. M. F., Brown, P. E., and Chambers, A. D. (1977) *Contrib. Mineral. Petrol.* **63,** 129–47.